Advances in Materials Research, *Vol. 8, No. 4 (2019) 275-293*
DOI: https://doi.org/10.12989/amr.2019.8.4.275

Experimental and numerical investigation on gas turbine blade with the application of thermal barrier coatings

Abdul Aabid *[1], Jyothi [2], Jalal Mohammed Zayan [1] and Sher Afghan Khan [1]

[1] *Department of Mechanical Engineering, Faculty of Engineering, International Islamic University Malaysia, P.O. Box No. 10, 50728, Kuala Lumpur, Malaysia*
[2] *Department of Aeronautical Engineering, Faculty of Engineering and Technology, Khaja Bandanawaz University, Rauza-I Buzurg, Kalaburagi (Gulbarga), 585104, Karnataka, India*

(*Received October 5, 2019, Revised December 27, 2019, Accepted January 20, 2020*)

Abstract. The engine parts material used in gas turbines (GTs) should be resistant to high-temperature variations. Thermal barrier coatings (TBCs) for gas turbine blades are found to have a significant effect on prolonging the life cycle of turbine blades by providing additional heat resistance. This work is to study the performance of TBCs on the high-temperature environment of the turbine blades. It is understood that this coating will increase the lifecycles of blade parts and decrease maintainence and repair costs. Experiments were performed on the gas turbine blade to see the effect of TBCs in different combinations of materials through the air plasma method. Three-layered coatings using materials INCONEL 718 as base coating, NiCoCrAIY as middle coating, and $La_2Ce_2O_7$ as the top coating was applied. Finite element analysis was performed using a two-dimensional method to optimize the suitable formulation of coatings on the blade. Temperature distributions for different combinations of coatings layers with different materials and thickness were studied. Additionally, three-dimensional thermal stress analysis was performed on the blade with a commercial code. Results on the effect of TBCs shows a significant improvement in thermal resistance compared to the uncoated gas turbine blade.

Keywords: materials; turbine blade; coatings; thermal analysis; finite element method; plasma spray

1. Introduction

In the development of science and technology, the need for aero engines with high performance is increasing rapidly. As we all know, the most efficient way to meet this need is to achieve a high inlet temperature of the gas turbine. High turbine inlet temperature can increase the stress level subsequently, and this affects the reliability and life of an engine. So, a material that can sustain high temperatures must be used to improve the turbine performance in an engine. The turbine blades have become limiting components for gas turbines. The turbine blades frequently use progressive materials such as superalloys and numerous dissimilar approaches of cooling; for example, internal air channels, boundary layer cooling, and TBCs. The TBCs materials find the most exceptional applications in fabulously sophisticated temperature mechanisms in aircraft engines due to high-temperature resistance and low thermal conductivity. The TBCs provides more

*Corresponding author, Ph.D., E-mail: abdul.aabid@live.iium.edu.my

http://www.techno-press.org/?journal=amr&subpage=5 ISSN: 2234-0912 (Print), 2234-179X (Online)

significant insulation characteristics; it can be an advantage for change in available temperature to the maximum temperature. The flow characteristics related to the cooling requirements influence the insulation properties of TBCs. Hence, to study more about TBCs literature, an extensive experimental study has been performed in the TBCs and TGO systems to identify the current challenges and research gap.

2. Literature review

Since the last four decades, TBC's system has been found suitable in high-temperature applications due to its high temperature resisting characteristics. Many types of research have been conducted on their performance evaluation, and the coating technology applied to them has proved to be more advantageous in improving their thermal properties. Aircraft gas turbine engine and power generation plants operate at high turbine inlet temperature or combustion temperature to obtain high thermal efficiency. It has been observed that when the parts made up of Nickel-base super alloy get in contact with flame, this superalloy has high resistance to heat. Evaluating the effects of compositional variations on the performance of TBC's system for airplane engine components, Stecura (1979) used Ni-base bond coatings and zirconium oxide layers as a fragment of ongoing exertion to grow TBC's system. This TBC's technique increased heat resistance. However, the delamination caused by the growth of TGO decreases the life of TBC's system (Lee *et al*. 2015). The CoNiCrAlY bond coats were used as TBC's system, deposited by cold gas-dynamic spray method. The oxidation behavior of this system was investigated under isothermal oxidation at 1000°C, 1100°C, and 1200°C for 8, 24, 50, and 100 h, respectively, and oxidation growth kinetics of TGO was determined (Karaoglanli *et al*. 2016).

The thermal conductivity of spark plasma sintered yttria-stabilized zirconia (YSZ) model, TBC's containing 10 or 20 vol.% of MoSi2 healing particles, was investigated using the laser flash method (Kulczyk-Malecka *et al*. 2016). TBC's crack surface and TGO formation layers at the interface were studies by performing their oxidation and thermal cycling tests (Doleker *et al*. 2018). Dautov *et al*. (2019) used the suspension plasma spraying technology for increasing the thermal and mechanical properties of the TBC's. Coating technology was also investigated from the detonation-gun-sprayed NiCrAlY, and 80Ni-20Cr coating applied to the alloy of X22CrMoV12-1 at 600°C for corrosion studies (Subramani *et al*. 2019). Rousseau *et al*. (2019) explained the progressive injection method for the repair of damaged thermal barrier technology. Miller (1997) advanced the application of low-risk turbine section TBC's from the laboratory and essential portion of engine design and useful to progressive air-cooled, super alloy mechanisms. Choi *et al*. (1999) studied the multi-layer TBC's on super-alloy substrates comprising of an inter-metallic bond coat. The TGO layer and a porous zirconia topcoat that affords thermal protection was also evaluated. Similar studies have been done in TBC's method that implemented multiple vanes using plasma spray (physical vapor deposition technology). Moreover, the preparation and distribution analysis was also explained (Mao *et al*. 2017). Rosler *et al*. (2001) calculated the mechanical loading of the TBC's or bond coat interface region for a TBC's coated superalloy specimen using an FE method. Aabid and Khan (2018) focused on the design of turbine blade and coating materials using a numerical approach, and experimentally tested a turbine blade with and without coatings at the high-temperature range.

Sadowski and Golewski (2012) investigated the effectiveness of the protection of turbine blades through TBC's and internal cooling under thermal shock cooling via ABAQUS simulation.

Sadowski and Pietras (2016) numerically analyzed a cooled turbine blade with various kinds of functionally graded thermal coatings to find the optimal material properties distribution of the functionally graded TBC's thereby avoiding the damage initiation and growth between TBCs and substrate. Moskalenko and Kozhevnikov (2016) also used the numerical analysis for the investigation of thermally stressed gas turbine elements, first stage power turbine blades, and cooling efficiency. Białas (2008) has made a similar approach to numerical simulation for crack development within atmospheric plasma spraying (APS) TBCs system. He modeled the thermally grown oxide (TGO) thickening and creep deformation of all system constituents. FE model of turbine blade coated with multi-layer-structure TBCs was developed, in which conjugate heat transfer analysis and the decoupled thermal-stress calculation method was adopted. The value closer to the actual temperature field was obtained the external flow field was performed and analyzed using three turbulence models: RNG k-ε, realizable k-ε, and SST k-ω turbulence model (Zhu *et al*. 2017). However, according to the numerical studies, most of the work has been done through the ABAQUS tool, and progressive cooling effects through the coating's material on blades were investigated.

Tang *et al*. (2015) studied the thermal-stresses and temperature distribution in different service stages with a two-dimensional model of a TBC's turbine blade. Ali and Janajreh (2015) numerical studied the various heat transfer configurations of jet impingement on a semi-circular surface. These configurations were compared for efficient heat transfer by achieving higher Nusselt number and lower surface temperature as convection heat, this has become the dominant phenomenon. Zhu *et al*. (2015) investigated the consequence of the morphology of TGO on the stress distribution under the growth of repeated thermal loading. A TBC's gas turbine blade was modeled using the FE method and coatings deposition process, high-temperature creeps, and elastic-plastic behavior were investigated. Hwang *et al*. (2016) reported the steady-state and unsteady-state conjugate heat transfer of a high-pressure gas turbine blade.

Furthermore, the solid and fluid domains were calculated by ANSYS simulation. Liu *et al*. (2016) investigated the insulation properties of TBC's by link flow and heat transfer analysis with the selection of a multi-layer blade. Li *et al*. (2017) investigated the changes in microstructure and properties of Nano-structured TBC's during thermal exposure to reveal the sintering mechanism operative in these coatings. Mafeed *et al*. (2012) performed the heat transfer analysis of pin fins of various geometries like circular, triangular, and rectangular, and thus found the optimum design. Moreover, it considered the fin with convective boundary tip and solved analytically the equation governing the one-dimensional heat conduction in the fin for obtaining the temperature distribution and heat transfer rate. Umair *et al*. (2018) studied the characteristic of heat dissipation rate, a variation of Nusselt number versus radial distance over the target surface. They found that the magnitude of the Nusselt number decreases gradually with the increase in the radial distance away from the jet.

Gentleman and Clarke (2004) examined the restrictions of phase compatibility with the thermally grown aluminum oxide. They studied the aging and degradation mechanism of a modern standard TBC's system and found that the advanced TBC's operating at higher temperatures and for very long durations in commercial aircraft applications need further developments (Bacos *et al*. 2011). Zhao *et al*. (2011) carried out pulsed thermography for non-destructive evaluation of as-sprayed APS TBC's and their microstructure revealed the essential information about defective position and degree; evidenced by their thermal images corresponding to subsurface pores and cracks. Proton microscopy scanning carried out to determine the distribution patterns of existing elements in the matrix of base alloy and the successive coatings and refurbished turbine blades by

(Kakuee *et al*. 2015).

Hernandez *et al*. (2009) investigated a fatigue cracks initiation in TBC's blade subjected to thermal gradient mechanical fatigue testing. The development of the cracks of interest, the thermo-mechanical response of the bond coat and the TGO were examined and quantified through FE analysis. Ogiriki *et al*. (2015) analyzed the performance-based creep life estimation model capable of predicting the impact of different forms of degradation on the creep life of gas turbines. The model comprises of performance, thermal, stress, and life estimation models. A high-pressure turbine blade as the life-limiting component of the gas turbine was investigated, and stress analysis of the plasma sprayed TBC's system using three-dimensional coating interfaces was done using the FE approach. Then, the three-dimensional coordinates of the coating surfaces were measured through the three-dimensional reconstruction of scanning electron microscope images (Kyaw *et al*. 2017). To evaluate whether the residual stresses related to failure are highly localized and may be enough for crack nucleation, but not for crack propagation and crack failure. A fracture mechanics approach was used, the cracks were modeled in the critical areas of the TBC's system and assessed using the modified crack closure integral method for determining the mode-dependent crack loading. The crack propagation capability was then predicted using a mix-mode failure criterion and proper fracture toughness data (Aktaa *et al*. 2005). Moon *et al*. (2015) investigated the thermal stress effect on the creep lifetime for a combustion liner in a gas turbine engine. For the calculation of the thermal stress of a combustion liner, the three-dimensional analysis was performed using an FE method.

Padture *et al*. (2002) reviewed the study of aircraft and industrial gas turbine engines, which has the most complex structure of TBC's, and it operates in the most demanding high-temperature environment. A similar review on the TBC's system and challenges on future research were also done by the authors (Bakan and Vaßen 2017, Ma and Ruggiero 2018, Saif *et al*. 2019). Hermosilla *et al*. (2009) overviewed the new program of modeling work, which was undertaken to understand the development of stresses due to the growth of the oxide layer. Kumar and Kandasubramanian (2016) reviewed various processing techniques and design methodologies for TBC's. The study focused mainly on particle technology and the inter-relationship between particle preparation, modification, and the resulting properties. To assist developments in advanced and novel TBC's for applications of engineering has been studied. Vardelle *et al*. (2016) reviewed thermal spray technology and explained its practices and progress in engineering applications. They divided the work into three main categories to express the challenges and recommendations. According to the review studied, it has been found that several studies have been carried out by the researchers on the TBC's system, and most of the work has been done through numerical simulations.

From the literature survey, it has been found that most of the work has been done through numerical methods using ANSYS, ABAQUS, and other relevant tools. However, experimental work was done by a few researchers. It is evident from the literature that the TBC's and TGO systems have been utilized for thermal analysis, stress analysis, and coating technology. Moreover, the TBC's regime is found to be favorable in failure and creep structure repair to increase the life of the structures. TGO system is beneficial in coatings technology as it improves the cooling effect of turbine blades subjected to high-temperature operating conditions. In addition, numerous materials have been used as coatings for turbine blades. In this work, the focus is on different combinations of the coating material and modeling of a turbine blade using the finite element method. The two-dimensional FE results, which were obtained from the simulation, were used for the validation of experimental study. The experimental, as well as simulation study, was performed only for one case. For this purpose, a three-dimensional gas turbine blade was designed

and modeled for structural and thermal loading conditions. Thus, this paper presents the design and analysis of TBC's by studying the steady-state conjugate heat transfer through a different layer, and the combination that provides maximum thermal resistance was determined.

3. Experimental work

Various procedures can be utilized to make TBCs on turbine blades. Some of the steps include coloration, masking, degreasing, vapor blasting, and heating. In the present study, the air plasma method (APS) is used to create laminates of TBCs layers in the gas turbine blade (Aabid and Khan 2018). The coating materials used in the study are isotropic, homogenous, and temperature independent.

The Initial coating was done by using INCONEL 718 superalloy with a thickness of 1 mm. The second layer bond coating was done by using a Nano-structural ceramic-metallic composite (NiCoCrAIY), with a thickness of 0.15 mm. The third and final layer coating was done using a ceramic composites-$La_2Ce_2O_7$ with a thickness of 0.09 mm. A gap of about 24 hours is given between each layer of coatings for proper application and curing purposes. The thickness of each coating material was measured after each application based on the applied quantity. Fig. 1 shows

Fig. 1 Coated blade

(a) (b)

Fig. 2 Gas turbine blade (a) Before Hear treatment; (b) After Hear treatment

the turbine blade after the coating. Initial thermal tests were carried out by heating the TBC coated turbine blades to 650 deg C for approximately 60 mins. TGO formation of about 0.01 mm was noticed during the inspection of the turbine blade after heating. The measurement of thermal conductivity of the TGO was found to be 4.0 W/m K. Figs. 2(a) and (b) represent the turbine blade without heat and with heating, respectively.

The temperature distribution through the cross-section of the blade material was measured with and without TBCs. Fig. 2(a) shows the turbine blade before heating. It can be observed that the color is grey before heating, and it turns bluish color after heating, as can be seen from Fig. 2(b). The temperature value decreased after the application of the coating.

4. Finite element modelling and analysis

4.1 Two-dimensional modelling

A two-dimensional (2D) numerical model is designed using the finite element method through the ANSYS Parametric design language (APDL) tool. Different coating layers are applied in a 2D model. A two-dimensional model of blade surface was designed, and the coatings of varying thicknesses and combinations were applied on its surface. Investigations were carried out by varying the coating material combinations. Simulations were also done by using higher temperature on the coatings to study the performance effect of coated materials.

4.1.1 Heat transfer analysis by changing coatings material on the laminates

Optimization of the TBC combinations was done on the laminated materials for the temperature distribution. In the present study, four different cases were simulated to optimize the combinations of coatings material with desired thicknesses. The thickness of the respective layer, along with their thermal conductivities, are mentioned. The film coefficient and the temperature of the turbine inlet gas is 2028 W/m^2k and 1373 K.

The thicknesses and thermal conductivities of coatings layers are; convective elements (hot gas) of 0.01 mm thickness. Topcoat ($La_2Ce_2O_7$) of 0.15 mm thickness and 0.65 W/m K of thermal conductivity. Bond coat (NiCoCrAlY) of 0.09 mm thickness and 17.0 W/m K of thermal conductivity. Superalloy (INCONEL 718) of 1 mm thickness and 25.0 W/m K of thermal conductivity.

4.1.2 Three-dimensional modelling of blade

A three-dimensional first-stage rotor blade in a gas turbine along with the periphery of the hub is designed using CATIA V5 shown in Fig. 3. The geometry of the turbine is drafted based on the dimension of the NASA rotor 37. Table 1 illustrates the dimension of the blade designed.

The TBCs are composed of three-layer coatings, a superalloy INCONEL 718 of 1 mm as a first coat. Next, a Nano-structured ceramic-metallic composite NiCoCrAIY as a bond coat of 0.09 mm. Lastly, the ceramic composite $La_2Ce_2O_7$ as a topcoat of 0.15 mm on the nickel alloy substrate. The materials properties are listed in table 2.

4.2 Meshing and boundary conditions

The initial condition of the blade consists of room temperature of 300 K, and the applied temperature in a blade section is 1373 K The film coefficient of the gas turbine inlet is 2028 w/m^2k

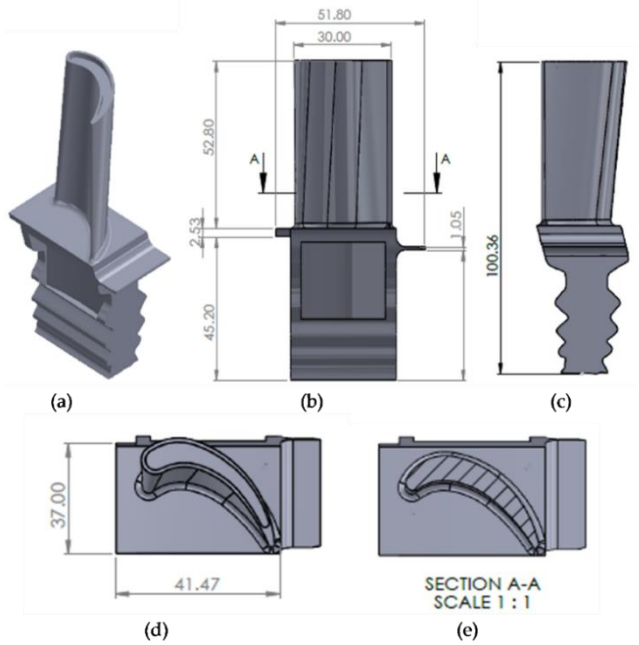

Fig. 3 FE model and dimension of a gas turbine rotor blade

Table 1 Dimensions of the gas turbine blade

Parameters	
Chord Length of Blade	30 mm
Height of Blade	52.80 mm
Total height (blade height + hub)	100.36 mm
Trailing edge Thickness	0.8 mm
Leading-edge Thickness	2 mm

Table 2 Material properties

Material properties	Topcoat	Initial coat	Bond coat	Substrate
Young's Modulus (GPa)	49	200	200	220
Density (kg/m^3)	5730	8220	7200	8908
Poisson's ratio	0.1	0.294	0.3	0.208
Thermal conductivity (W/m K)	0.65	25	17	11.3
Thermal expansion coefficient (×10-6/K)	9.0	16.2	13.6	14

as per the two-dimensional studies.

The geometrical model was imported into the hyper mesh. Structural mesh with tetrahedron elements was used. Insignificant geometrical shapes were eliminated to avoid meshing complications, as shown in Fig. 5. The minimal mesh sizes of the blade's cross-section (airfoil)

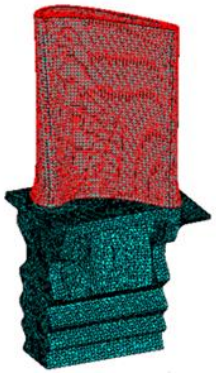

Fig. 4 Mesh model of turbine blade along with hub heat transfer analysis

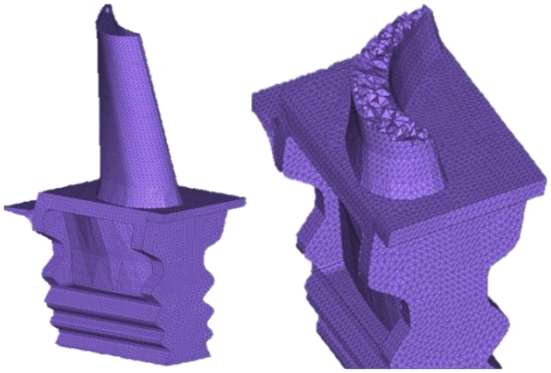

Fig. 5 FE mesh of a gas turbine blade

and platform were chosen as 0.8 mm; the total number of elements was approximately 1,19,885, with 2,37,402 nodes. The meshing of the TBCs was done using 3D shell elements.

The three layers of TBC's over the nickel superalloy substrate of turbine blade have meshed independently with different thicknesses. The boundary conditions are defined, and the turbine blade is analyzed. The boundary conditions are determined by considering the surface of the blade; the blade consists of a total of three surfaces (top, bottom, and blade). The bottom face of the hub is considered as a fixed end, and the top surface of the blade referred to the free end.

The effect of temperature and induced stresses on the turbine blade were investigated through the analysis. Thermal analysis has been carried out to examine the direction of the temperature flow due to the thermal loading. A thermal-structural analysis was done to find the stresses and displacements of the turbine blade. The details of the thermal barrier coatings are shown in Fig. 6.

4.3 Mesh independence study

Mesh independence study was done by analyzing the thermal-stresses on the 3D blade model with TBCs the different mesh types that were observed by varying the element size. Simulations were done on a PC that runs on Intel(R) Core i7-3770 CPU @ 3.40 GHz, 16.0 GB RAM, and Windows-10 64-bit operating system structured grid was used to mesh the blade, 1st coat, 2nd coat,

and 3rd coat. Unstructured meshing was used for the design of the hub of the blade. Table 3 illustrates the mesh size for all the elements Von Mises stress value was improved with a slight variation of the mesh, leading to a maximum relative difference of 5 percent. This evaluation shows that the medium mesh is more effective with about half the run time compared to the fine mesh, and hence, this mesh size was used for the rest of the simulations.

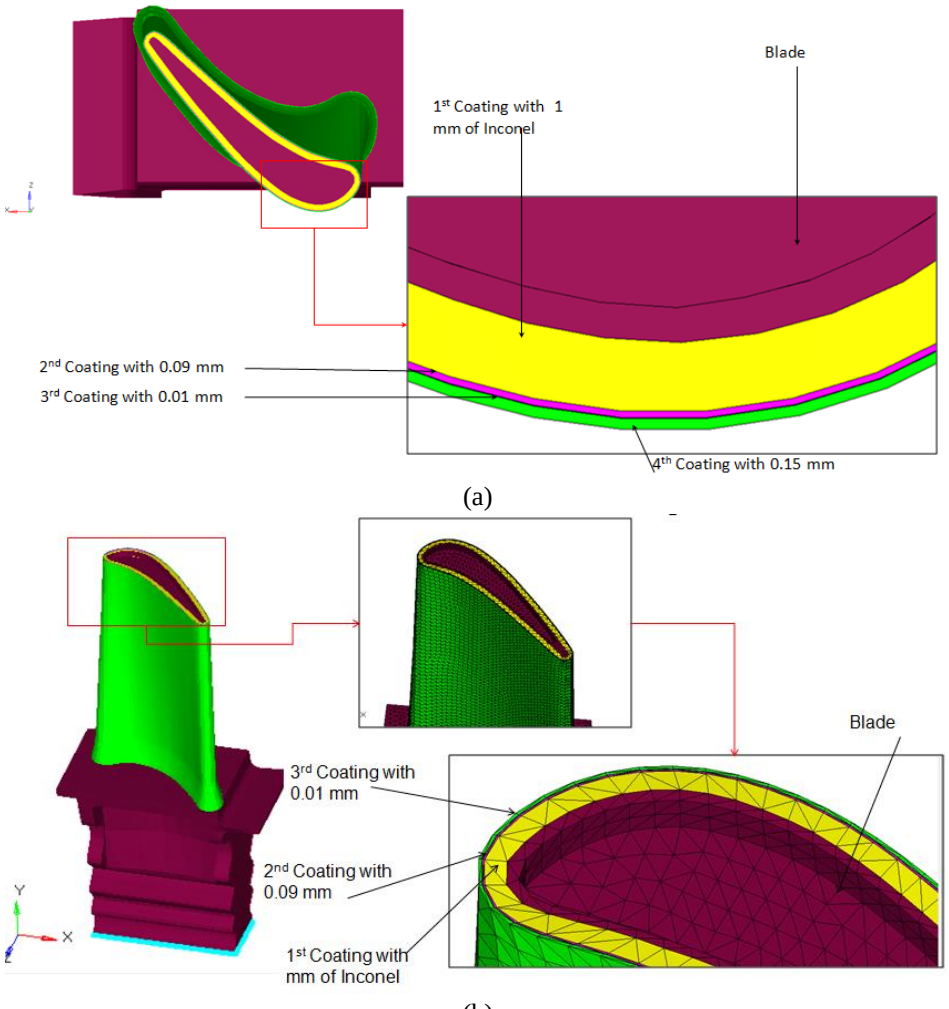

Fig. 6 Coatings a gas turbine blade (a) FE Model (b) FE Mesh

Table 3 Mesh independence test

Mesh type	No. of elements	CPU runtime (seconds)	Von Mises stress (GPa)
Coarse	68,920	1309	4.32
Medium	1,19,885	2644	3.09
Fine	1,93,981	4891	2.92

5. Results and discussion

The results obtained from experiments and numerical methods are discussed based on thermal and thermal and structural analysis.

5.1 Experimental results

The present experimental work is only limited to the coating's effects and thermal conductivity test with and without coating, which is shown in Figs. 1 and 2. The study includes the fabrication of the turbine blade with the TBCs materials based on the results obtained from heat transfer analysis for different coatings materials. The turbine blade of nickel superalloy is used as the experimental specimen's material, which has the high-temperature resisting capacity in the hot component, which in turn increases the service life of the blade. The air plasma method was used for the fabrication of the TBCs on the gas turbine blade, which consists of three layers of coatings effects; initial coat, bond coat, and topcoat.

Finally, the obtained experimental result for the single case of coatings material has been found 455 K of TBCs temperature in thermal conductivity test. Moreover, our experimental work is limited to only two instances because of two specimens; the first used without the TBCs test and the second user with TBCs.

5.2 Two-dimensional results

Four different cases have been taken into consideration, in case one the topcoat is $La_2Zr_2O_7$ and superalloy is INCONEL 718, the obtained result shows that the resistance of temperature difference on the blade is up to 1400 K which is better than the un-coated gas turbine blade. Next, in case two, the topcoat of 3YSZ and superalloy of chromium steel, the heat transfer shows that difference in the temperature is the lowest temperature of 500 K and the highest temperature of 1400 K. For the third case, the topcoat is 3YSZ, and the superalloy is INCONEL 625. The obtained results for the third case confirm that the modification of the superalloy from chromium steel to INCONEL 625; the temperature variations are significant, but the range of the temperature is similar; nevertheless, differences in average temperature (at node 3, 4 and 5).

Finally, in the last case (fourth), the topcoat of $La_2Zr_2O_7$ and superalloy of INCONEL 718 are used. It is coated with $La_2Zr_2O_7$, the observation based on the earlier (case three), and current (case four) results show that the temperature variation again changed. Fig. 7 demonstrates the evaluation of the different combinations of coatings material for the topcoat to the superalloy. The results show that the TBCs blade can resist the temperature up to 1400 K, which far better than the un-coated blade, and the minimum is 250 K.

Consideration of all four cases and different nodes at node five of case one, the value of temperature found close to the obtained experimental result, which is illustrated in table 4. Therefore, to validate the experimental result, the numerical result of node five for case one has less discrepancy.

Table 4 Mesh independence test

Heat treatment	Experimental	Numerical	Relative error (%)
650°C	455 K	446 K	1.978

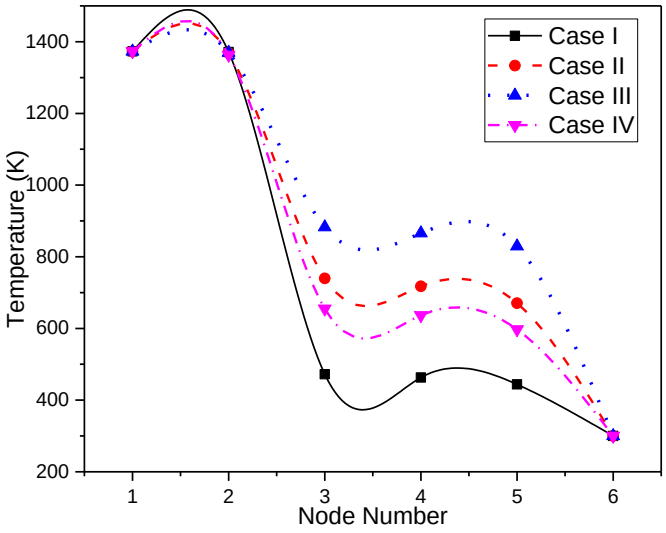

Fig. 7 Nodal results

5.3 Three-dimensional results

A three-dimensional FE model has been used to obtain a different interpretation of a gas turbine blade with and without TBCs. In this study, considered the only a single case of coatings material, which is the case one because of previous analysis it found close to the experimental work. Therefore, it is selected for further investigation (three-dimensional analysis).

5.3.1 Thermal-structural analysis of gas turbine blade without TBCs

The thermal-structural analysis was performed for the turbine blade with the same ANSYS mechanical APDL software. The FE method is used for the thermal-structural analysis to calculate the deformation, von-misses, and the principal stresses on a turbine blade with and without TBCs.

Figs. 8(a) and (b) show the analysis of thermal gradient and thermal flux on the turbine blade without the TBCs, from the figures it is seen the maximum thermal gradient, and thermal flux are found at the attachment of the turbine blade to the hub of the blade. This implies that the temperature gradient is critical at the location of the high-stress area; therefore, at the edge of the attached blade to the hub, we found the higher value of the thermal gradient compared to other surfaces of the blade and hence; this phenomenon is like thermal flux.

Fig. 9 shows the maximum displacement due to thermal expansion on the turbine blade without coatings material, this is seen at the tip of the blade, and there is a gradual decrease in the displacement from tip to the root of the blade. It means that the displacement is higher at the free end as compared to a fixed end, which is almost lower at the hub of the blade, that can be seen through a contour color (blue).

Fig. 10 shows the structural failure due to the thermal forces on the turbine blade in terms of von Mises stresses; the maximum stress is noticed on the hub of a turbine blade. Therefore, the structural failure may occur at the hub rather than on the blade, when the thermal forces are applied. However, the high-stress area is found between the blade and the hub. Therefore, when the blade takes the thermal load, structural loads are more in the high-stress area. In this case, the

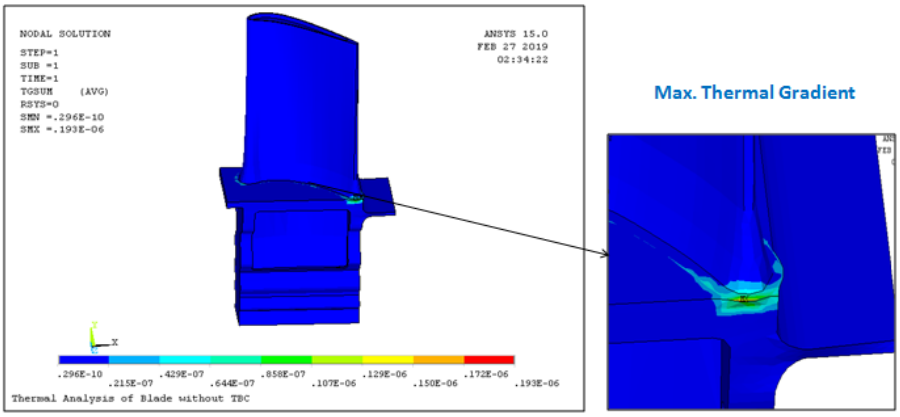

(a)

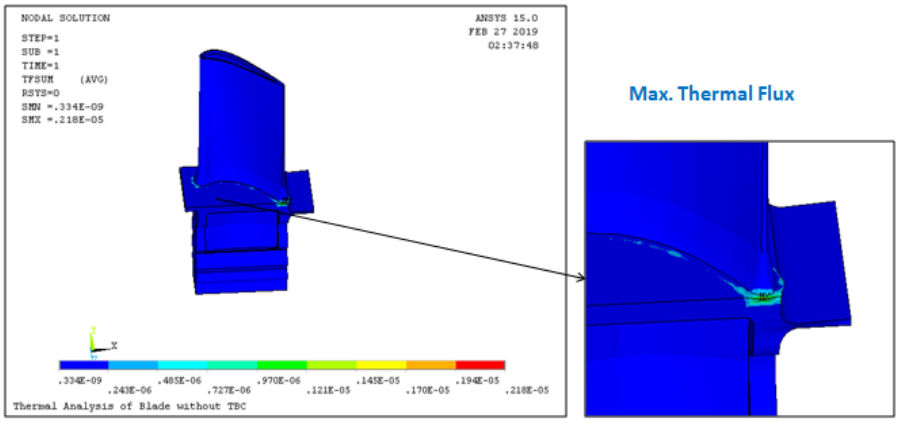

(b)

Fig. 8 Turbine blade without coatings (a) Max thermal gradient; (b) Max thermal flux

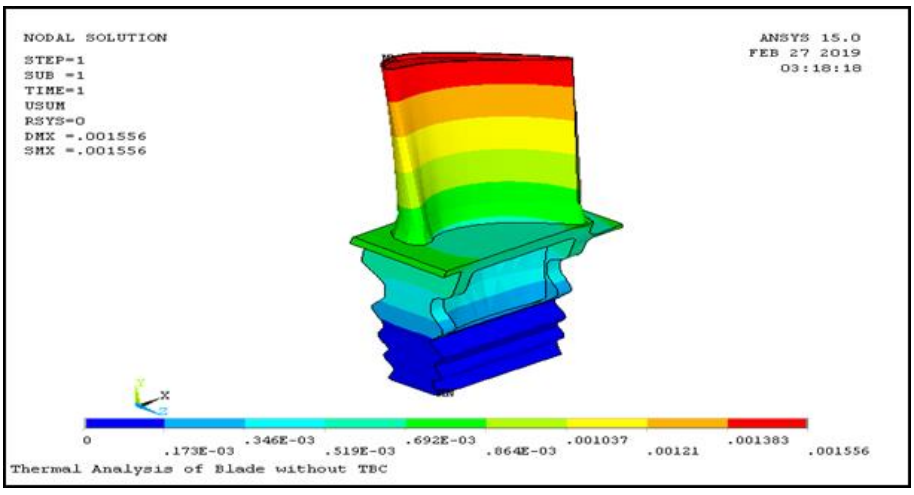

Fig. 9 Max displacement due to thermal expansion on the turbine blade without coatings

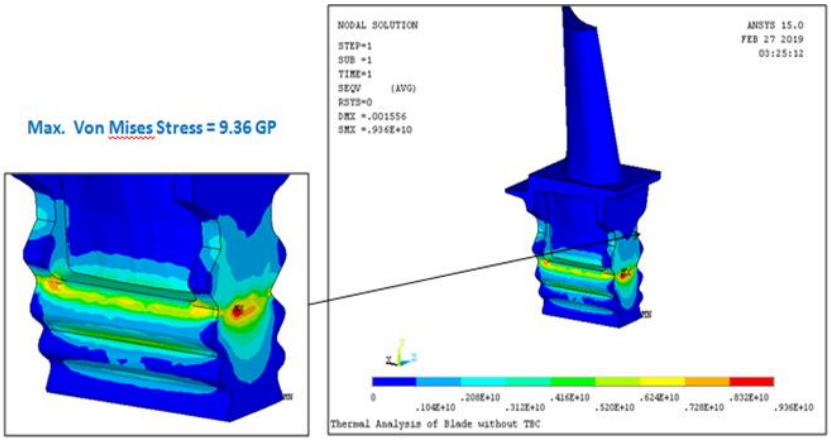

Fig. 10 Max von Mises stress on the turbine blade without coatings

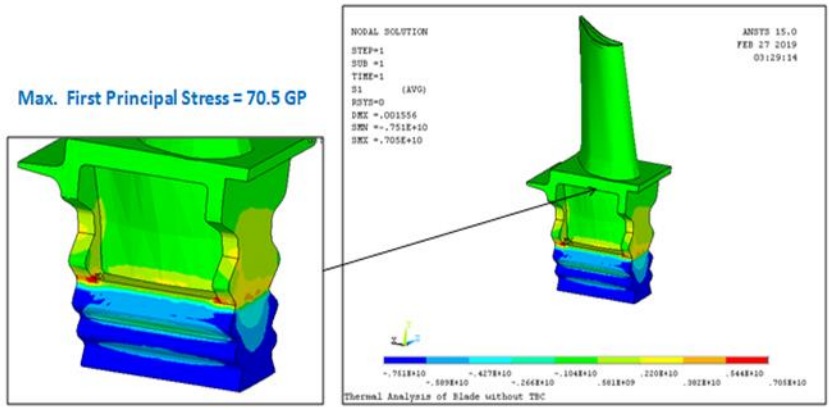

Fig. 11 Max first principle stress on the turbine blade without coatings

high-stress area is at the hub because of the fixed edge in the applied boundary conditions.

It is also noticed that the results for the principal stresses for a non-coated blade (Fig. 11), found that the results are not similar as compared to the von Mises stresses. The results of von Mises stress accounts for higher values in one location (red contour color), and other positions are constant (blue contour color). Still, for the principal stress, it is lower at the fixed surface of the hub (blue contour color), medium in other locations of the blade (green contour color), and higher at the high-stress area (red contour color).

5.3.2 Thermal-structural analysis of gas turbine blade with TBCs

A similar set of study is done for the turbine blade with TBCs material, for the comparison of the turbine blade without TBCs material. Figs. 12(a) and (b) show the thermal gradient and thermal flux analysis on the turbine blade with the TBCs. From the statistics, it is seen that the maximum thermal gradient and thermal flux is seen on the turbine blade rather than at the attachment of the blade and the hub. This is due to the presence of TBC material; the thermal

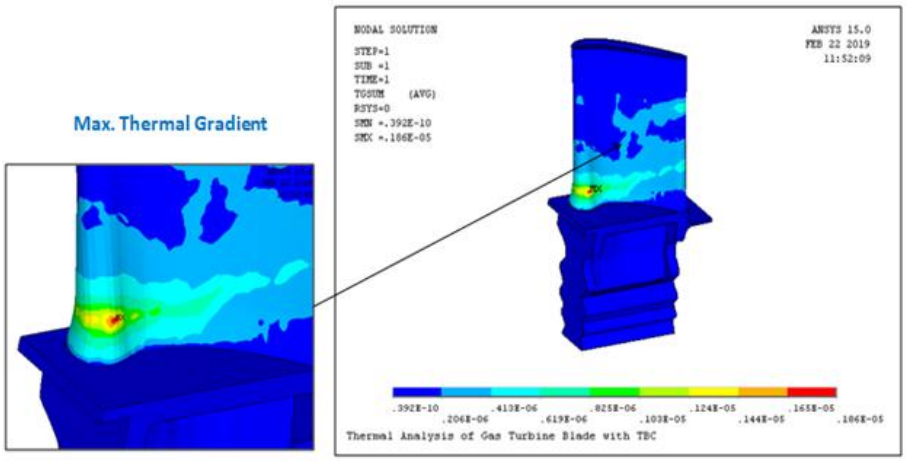

(a)

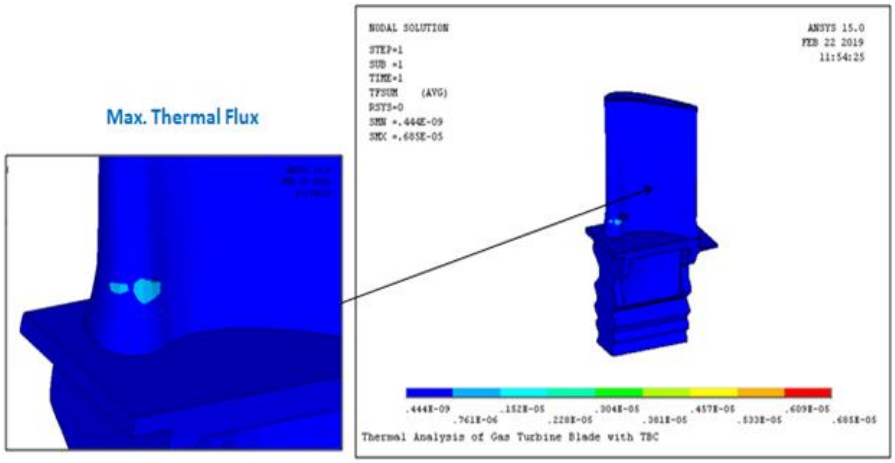

(b)

Fig. 12 Turbine blade with coatings (a) Max thermal gradient; (b) Max thermal flux

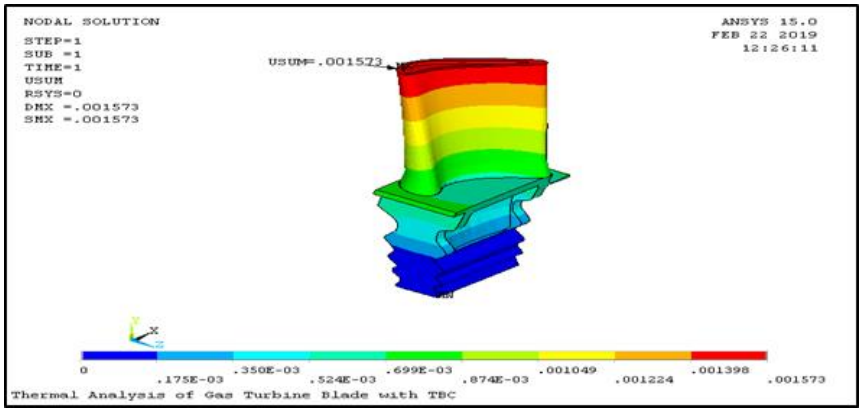

Fig. 13 Max displacement due to thermal expansion on the turbine blade with coatings

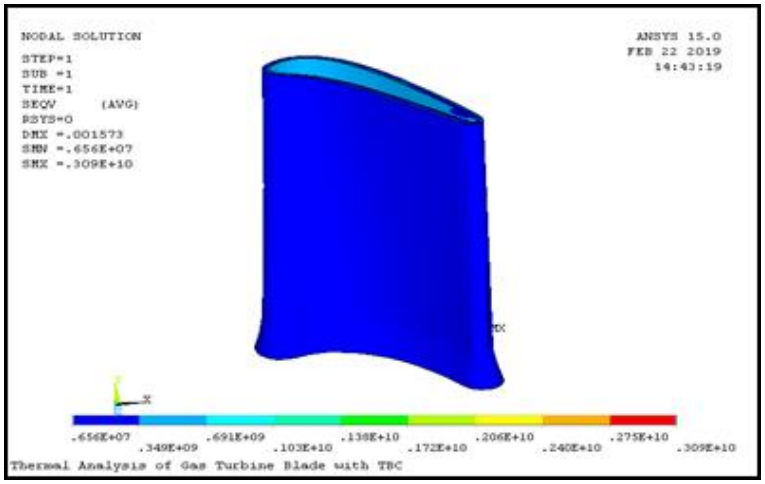

Fig. 14 Max von Mises stress on the turbine blade with coatings

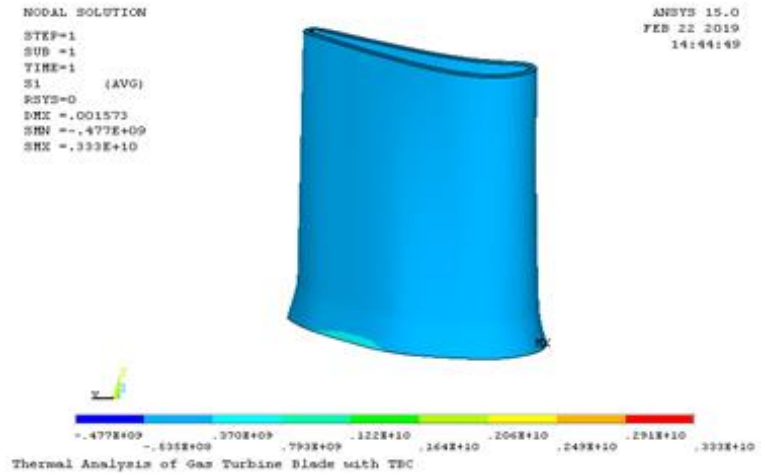

Fig. 15 Max first principal stress on the turbine blade with coatings

Table 5 Comparison of the turbine blade results for non-TBCs and TBCs

Component	Max displacement max	Von Mises stress	Max first principal stress
Without TBCs coat	0.001556 m	9.36 GPa	70.5 GPa
With TBCs coat	0.001556 m	3.09 GPa	3.33 GPa

gradient occurs at different parts of the component to expand by an unusual magnitude, unlike the case of thermal flux.

Fig. 13 shows the maximum displacement due to thermal expansion on the turbine blade with TBC material. The maximum displacement is seen at the tip of the blade, and there is a gradual decrease in the displacement from tip to the root of the blade, the maximum displacement with and

without TBC materials shows the similar results.

Figs. 14 and 15 illustrations the structural failure due to the thermal forces on the turbine blades in term of von Mises stress and principal stress for a blade with TBCs material. The maximum stress is noticed near the hub of a turbine blade, as compared to the stressed with and without TBC material, there is a considerable change in the stress values, and for excellent results are obtained for a turbine blade with TBCs material.

The comparison of the results which are obtained for the thermal-structural analysis without and with TBCs coat on the turbine blade is tabulated in Table 5. The max displacement due to thermal expansion on the turbine blade without TBCs and with TBCs, are as shown in Figs. 9 and 13, both show a similar result of 0.001556 m.

6. Conclusions

Experimental and numerical study was carried out for testing the temperature distribution of the gas turbine blades with and without TBCs. A finite element analysis was done to validate the experimental results for a single case using TBCs. The discrepancy between the experimental and the FEA simulation (numerical study) was about 1.978%. Four different cases of varying coatings were simulated on the blade surface. The TBCs material combinations were selected based on the heat transfer analysis on the blade. The coatings on the blade were interchanged, and the results were compared. The two-dimensional model analysis was used for thermal analysis, whereas three-dimensional model analysis was used for thermal-structural analysis with and without TBCs. The coating, combined with the highest operational temperature resistance, was selected for three-dimensional thermal-structural finite element analysis. From the results, it was determined that TBCs are an ideal form of applicants for high-temperature resistance in turbine blades. It was further determined that interchanging the application of TBCs material on the surface of turbine blades results in varying heat resistant characteristics. The three-dimensional analysis also proves that the application of TBCs on the turbine blades provides superior structural protection on the blades, which increases its service life with higher operating temperatures.

References

Aabid, A. and Khan, S.A. (2018), "Optimization of heat transfer on thermal barrier coated gas turbine blade related", *Proceedings of IOP Conference Series*: *Materials Science and Engineering*, **370**, 1-9. https://doi.org/10.1088/1757-899X/370/1/012022

Aktaa, J., Sfar, K. and Munz, D. (2005), "Assessment of TBC systems failure mechanisms using a fracture mechanics approach", *Acta Materialia*, **53**(16), 4399-4413. https://doi.org/10.1016/j.actamat.2005.06.003

Al Ali, A.R. and Janajreh, I. (2015), "Numerical simulation of turbine blade cooling via jet impingement", *Energy Procedia*, **75**, 3220-3229. https://doi.org/10.1016/j.egypro.2015.07.683

Bacos, M.P., Dorvaux, J.M., Lavigne, O., Mévrel, R., Poulain, M., Rio, C. and Vidal-Setif, M.H. (2011), "Performance and degradation mechanisms of thermal barrier coatings for turbine blades : A review of onera activities", *J. Aerosp. Lab*, **3**, 1-11.

Bakan, E. and Vaßen, R. (2017), "Ceramic top coats of plasma-sprayed thermal barrier coatings: materials, processes, and properties", *J. Thermal Spray Technol.*, **26**(6), 992-1010. https://doi.org/10.1007/s11666-017-0597-7

Białas, M. (2008), "Finite element analysis of stress distribution in thermal barrier coatings", *Surf. Coatings Technol.*, **202**(24), 6002-6010. https://doi.org/10.1016/j.surfcoat.2008.06.178

Choi, S.R., Hutchinson, J.W. and Evans, A.G. (1999), "Delamination of multilayer thermal barrier coatings", *Mech. Mater.*, **31**(7), 431-447. https://doi.org/10.1016/S0167-6636(99)00016-2

Dautov, S.S., Shornikov, P.G., Rezyapova, L.R. and Akhatov, I.S. (2019), "Increasing thermal and mechanical properties of thermal barrier coatings by suspension plasma spraying technology", *J. Phys.: Conference Series*, **1281**, 1-4. https://doi.org/10.1088/1742-6596/1281/1/012008

Doleker, K.M., Ozgurluk, Y. and Karaoglanli, A.C. (2018), "Isothermal oxidation and thermal cyclic behaviors of YSZ and double-layered YSZ/La2Zr2O7 thermal barrier coatings (TBCs)", *Surf. Coatings Technol.*, **351**, 78-88. https://doi.org/10.1016/j.surfcoat.2018.07.069

Gentleman, M.M. and Clarke, D.R. (2004), "Concepts for luminescence sensing of thermal barrier coatings", *Surf. Coatings Technol.*, **188-189**, 93-100. https://doi.org/10.1016/j.surfcoat.2004.08.005

Hermosilla, U., Jones, I.A., Hyde, T.H., Thomson, R.C. and Karunaratne, M.S.A. (2009), "Finite element modeling of the development of stresses in thermal barrier coatings", *Proceedings of 2009 International Conference on Sustainable Power Generation and Supply*, 1-7. https://doi.org/10.1109/SUPERGEN.2009.5348018

Hernandez, M.T., Karlsson, A.M. and Bartsch, M. (2009), "On TGO creep and the initiation of a class of fatigue cracks in thermal barrier coatings", *Surf. Coatings Technol.*, **203**(23), 3549-3558. https://doi.org/10.1016/j.surfcoat.2009.05.018

Hwang, S., Son, C., Seo, D., Rhee, D.-H. and Cha, B. (2016), "Comparative study on steady and unsteady conjugate heat transfer analysis of a high-pressure turbine blade", *Appl. Thermal Eng.*, **99**, 765-775. https://doi.org/10.1016/j.applthermaleng.2015.12.139

Kakuee, O., Fathollahi, V., Oliaiy, P., Agha-Aligol, D. and Lamehi-Rachti, M. (2015), "Ion beam analysis of gas turbine blades: Evaluation of refurbishment quality", *Bull. Mater. Sci.*, **38**(2), 511-516. https://doi.org/https://doi.org/10.1007/s12034-015-0867-2

Karaoglanli, A.C., Turk, A. and Ozdemir, I. (2016), "Isothermal oxidation behavior and kinetics of thermal barrier coatings produced by cold gas dynamic spray technique", *Surf. Coatings Technol.*, **318**, 72-81. https://doi.org/10.1016/j.surfcoat.2016.12.021

Kulczyk-Malecka, J., Zhang, X., Carr, J., Carabat, A.L., Sloof, W.G., Van Der Zwaag, S., Cernuschi, F., Nozahic, F., Monceau, D., Estournès, C. and Withers, P.J. (2016), "Influence of embedded $MoSi_2$ particles on the high-temperature thermal conductivity of SPS produced yttria-stabilised zirconia model thermal barrier coatings", *Surf. Coatings Technol.*, **308**, 31-39. https://doi.org/10.1016/j.surfcoat.2016.07.113

Kumar, V. and Kandasubramanian, B. (2016), "Processing and design methodologies for advanced and novel thermal barrier coatings for engineering applications", *Particuology*, **27**, 1-28. https://doi.org/10.1016/j.partic.2016.01.007

Kyaw, S., Jones, A., Jepson, M.A.E., Hyde, T. and Thomson, R.C. (2017), "Effects of three-dimensional coating interfaces on thermo-mechanical stresses within plasma spray thermal barrier coatings", *Mater. Des.*, **125**, 189-204. https://doi.org/10.1016/j.matdes.2017.03.067

Lee, J.-M., Song, H., Kim, Y., Koo, J.-M. and Seok, C.-S. (2015), "Evaluation of thermal gradient mechanical fatigue characteristics of the thermal barrier coating, considering the effects of thermally grown oxide", *Int. J. Precision Eng. Manuf.*, **16**(7), 1675-1679. https://doi.org/10.1007/s12541-015-0220-0

Li, G.-R., Yang, G.-J., Li, C.-X. and Li, C.-J. (2017), "A comprehensive mechanism for the sintering of plasma-sprayed nanostructured thermal barrier coatings", *Ceram. Int.*, **45**(12), 9600-9615. https://doi.org/10.1016/j.ceramint.2017.04.083

Liu, J.H., Liu, Y.B., He, X. and Liu, L. (2016), "Study on TBCs insulation characteristics of a turbine blade under serving conditions", *Case Studies in Thermal Engineering*, **8**, 250-259. https://doi.org/10.1016/j.csite.2016.08.004

Ma, X. and Ruggiero, P. (2018), "Practical aspects of suspension plasma spray for thermal barrier coating on potential gas turbine components", *J. Thermal Spray Technol.*, **27**(4), 591-602. https://doi.org/10.1007/s11666-018-0700-8

Mafeed, M.P., Salman Ali, M., Prabin, C., Ramis, M.K., Ali Baig, M.A. and Khan, S.A. (2012), "Optimum

length for pin fins used in electronic cooling", *Appl. Mech. Mater.*, **110-116**, 1667-1673. https://doi.org/10.4028/www.scientific.net/AMM.110-116.1667

Mao, J., Liu, M., Deng, C.G., Deng, C.M., Zhou, K.S. and Deng, Z.Q. (2017), "Preparation and distribution analysis of thermal barrier coatings deposited on multiple vanes by plasma spray-physical vapor deposition technology", *J. Eng. Mater. Technol., Transactions of the ASME*, **139**(4), 1-7. https://doi.org/10.1115/1.4036584

Miller, R.A. (1997), "Thermal barrier coatings for aircraft engines: history and directions", *J. Thermal Spray Technol.*, **6**(1), 35-42. https://doi.org/10.1007/BF02646310

Moon, H., Kim, K.M., Jeon, Y.H., Shin, S., Park, J.S. and Cho, H.H. (2015), "Effect of thermal stress on creep lifetime for a gas turbine combustion liner", *Eng. Fail. Anal.*, **47**, 34-40. https://doi.org/10.1016/j.engfailanal.2014.10.004

Moskalenko, A.B. and Kozhevnikov, A.I. (2016), "Estimation of gas turbine blades cooling efficiency", *Procedia Eng.*, **150**, 61-67. https://doi.org/10.1016/j.proeng.2016.06.716

Ogiriki, E.A., Li, Y.G., Nikolaidis, T., Isaiah, T.E. and Sule, G. (2015), "Effect of fouling, thermal barrier coating degradation, and film cooling holes blockage on gas turbine engine creep life", *Procedia CIRP*, **38**, 228-233. https://doi.org/10.1016/j.procir.2015.07.017

Padture, N.P., Gell, M. and Jordan, E.H. (2002), "Thermal barrier coatings for gas-turbine engine applications", *Review*: *Mater. Sci.*, **296**(5566), 280-284. https://doi.org/10.1126/science.1068609

Rösler, J., Bäker, M. and Volgmann, M. (2001), "Stress state and failure mechanisms of thermal barrier coatings: Role of creep in thermally grown oxide", *Acta Materialia*, **49**(18), 3659-3670. https://doi.org/10.1016/S1359-6454(01)00283-X

Rousseau, F., Quinsac, A., Morvan, D., Bacos, M.P., Lavigne, O., Rio, C., Guinard, C. and Chevillard, B. (2019), "A new injection system for spraying liquid nitrates in a low power plasma reactor: Application to local repair of the damaged thermal barrier coating", *Surf. Coatings Technol.*, **357**, 195-203. https://doi.org/10.1016/j.surfcoat.2018.09.069

Sadowski, T. and Golewski, P. (2012), "The analysis of heat transfer and thermal stresses in thermal barrier coatings under exploitation", *Defect Diffusion Forum*, **326-328**, 530-535. https://doi.org/10.4028/www.scientific.net/DDF.326-328.530

Sadowski, T. and Pietras, D. (2016), "Heat transfer process in jet turbine blade with functionally graded thermal barrier coating", *Solid State Phenomena*, **254**, 170-175. https://doi.org/10.4028/www.scientific.net/SSP.254.170

Saif, M., Mullick, P. and Imam, A. (2019), "Analysis and structural design of various turbine blades under variable conditions : A review", *Adv. Mater. Res.*, **8**(1), 11-24. https://doi.org/https://doi.org/10.12989/amr.2019.8.1.011

Stecura, S. (1979), "Effects of compositional change on the performance of a thermal barrier coating system", *Proceedings of the 3rd Annual Conference on Composite and Advanced Materials*, Merritt Island, FL, USA, January.

Subramani, P., Padgelwar, N., Shetty, S., Pandit, A., Sreenivasulu, V., Arivazhagan, N., Duoli, W.U. and Manikandan, M. (2019), "Hot corrosion studies on detonation-gun-sprayed NiCrAlY and 80Ni–20Cr coatings on alloy X22CrMoV12-1 at 600°C", *Transact. Indian Inst. Metals*, 20-23. https://doi.org/10.1007/s12666-019-01567-6

Tang, W.Z., Yang, L., Zhu, W., Zhou, Y.C., Guo, J.W. and Lu, C. (2015), "Numerical simulation of temperature distribution and thermal-stress field in a turbine blade with multilayer-structure tbcs by a fluid-solid coupling method", *J. Mater. Sci. Technol.*, **32**, 452-458. https://doi.org/10.1016/j.jmst.2016.03.009

Umair, S.M., Alrobaian, A.A. and Khan, S.A. (2018), "Numerical investigation of critical range for the occurrence of secondary peaks in the nusselt distribution curve", *CFD Letters*, **1**(1), 12-27.

Vardelle, A., Moreau, C., Akedo, J., Ashrafizadeh, H., Berndt, C.C., Berghaus, J.O., Boulos, M., Brogan, J., Bourtsalas, A.C., Dolatabadi, A. and Dorfman, M. (2016), "The 2016 Thermal spray roadmap", *J. Thermal Spray Technol.*, **25**(8), 1376-1440. https://doi.org/10.1007/s11666-016-0473-x

Zhao, S., Zhang, C., Wu, N. and Wang, H. (2011), "Quality evaluation for air plasma sprays thermal barrier

coatings with pulsed thermography", *Progress in Natural Science*: *Mater. Int*., **21**(4), 301-306. https://doi.org/10.1016/S1002-0071(12)60061-6

Zhu, W., Cai, M., Yang, L., Guo, J.W., Zhou, Y.C. and Lu, C. (2015), "The effect of morphology of thermally grown oxide on the stress field in a turbine blade with thermal barrier coatings", *Surf. Coatings Technol*., **276**, 160-167. https://doi.org/10.1016/j.surfcoat.2015.06.061

Zhu, W., Wang, J.W., Yang, L., Zhou, Y.C., Wei, Y.G. and Wu, R.T. (2017), "Modeling and simulation of the temperature and stress fields in a 3D turbine blade coated with thermal barrier coatings", *Surf. Coatings Technol*., **315**, 443-453. https://doi.org/10.1016/j.surfcoat.2017.03.012

CC